2nd International Seminar On "Utilization of Non-Conventional Energy Sources for Sustainable Development of Rural Areas
ISNCESR'16
17th & 18th March 2016

Mode-Division Multiplexing Over Few-Mode Fiber Using Coherent 6×6 MIMO Processing

Anuja Mishra[1] and Sharad Mohan Shrivastava[2]

[1]FET-SSTC, Bhilai
anujamishra.10@gmail.com

[2]FET-SSTC, Bhilai
sharad.stva04@gmail.com

Abstract— The objective of this paper is to make readers understand the key terms related to optical fiber specifically few-mode fiber to help them carry out further research work. With the increasing demand for faster transmission systems, optical fiber communication system requirement is increasing day by day. As we know that the capacity limits of single mode fiber is almost reached its maxima, Space division multiplexing can be helpful for increasing the data rate requirement. In this paper, we understood the transmission of 6 spatial and polarization modes, each carrying quadrature-phase-shift-keyed channels over few-mode fiber keeping lower differential group delay. The detection of these channels is being carried out using coherent detection namely MIMO DSP. The 6×6 impulse-response matrix representation of few-mode fiber is presented, revealing the coupling characteristics between the modes.

Index Terms—Mode-multiplexing, Multiple Input Multiple Output (MIMO), Digital Signal Processing (DSP), Coherent Communication, multi-mode fiber.

1. Introduction

Single-mode fibers (SMFs) have been successfully exploited for long-distance optical transmission for over decades, at the same time their capacity continuously grew by three orders of magnitudes. The growth was improved by the successive introduction of wavelength division multiplexing (WDM) technique, polarization division multiplexing (PDM)technique , and higher-order modulation formats[1] known. Eventhough the capacity of SMFs is now approaching the limits imposed and calculated by the combination of Shannons information theory and nonlinear fiber effects[2]. In order to continue to grow the capacity and fulfill demands, a new dimension is now demanded and it has been suggested[3] that space-division multiplexing (SDM) be utilised as a technique for enhancement in capacity in optical transmission systems. In SDM, spatially distinct paths are used to transmit multiple channels, and if realized over a single fiber, SDM offers a significant potential for cost-, space- and energy savings[4].

SDM over a single fiber can be achieved in 2 different ways. The very first technique consists of using waveguides that support multiple distinct waveguide modes, such as in a multimode optical fiber (MMF). Earlier attempts of SDM over MMF [5]-[8] were limited in lower transmission distance and bandwidth, because the waveguide modes supported could not be selectively excited and detected and also because of the increased modal differential group delay (DGD) present in standard multimode fiber. Most recently transmission distance and bandwidth has been increased and enhanced by using few-mode fibers (FMFs) [9]-[14] which are MMF that support only a small and fixed number of waveguide modes. In this work the FMF transmission distance is further extended up to 137 km at 240 Gbps single wavelength channel bandwidth [15].

For such a transmission distance significant crosstalk between all modes offered by the FMF can be observed, and MIMO DSP for crosstalk reduction is required.
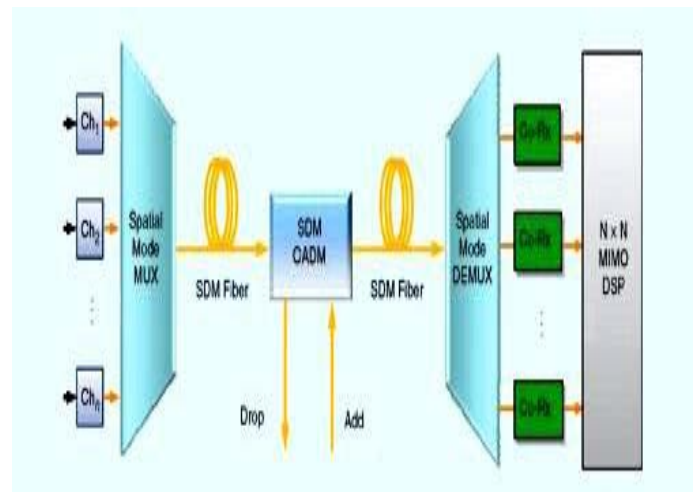

Fig. 1. N×N coherent SDM transmission based on MIMO DSP.

The second technique to implement SDM consists of multiple spatially distinct parallel waveguides formed and consisted inside the fiber. The simplest implementation is given by the multi-core fiber (MCF), and consists of multiple cores distributed and placed across the fiber section. In this technique, it is desirable to reduce the crosstalk between cores so that the individual cores can be considered as individual channels, thus greatly simplifying the communication system design and modelling. Even though the cores are spatially separated, achieving low crosstalk between cores for long haul transmission, can be a challenging task because the light is not completely confined and constricted in the cores of fiber.

However recently low crosstalk 7-core MCFs have been

demonstrated [16]-[17] using core spacing of >45 m and non-standard cladding diameters>150 m. In this work we show that the fiber design can be drastically simplified, and the spacing between cores reduced to < 30 m if crosstalk is allowed and subsequently undone by multiple-input multiple-output (MIMO) digital signal processing (DSP). Despite having large crosstalk, transmission distance have been improved apparently.

The general method to perform SDM transmission over FMF or CCF in the presence of crosstalk or coupling between the SDM channels is shown in Fig. 1.
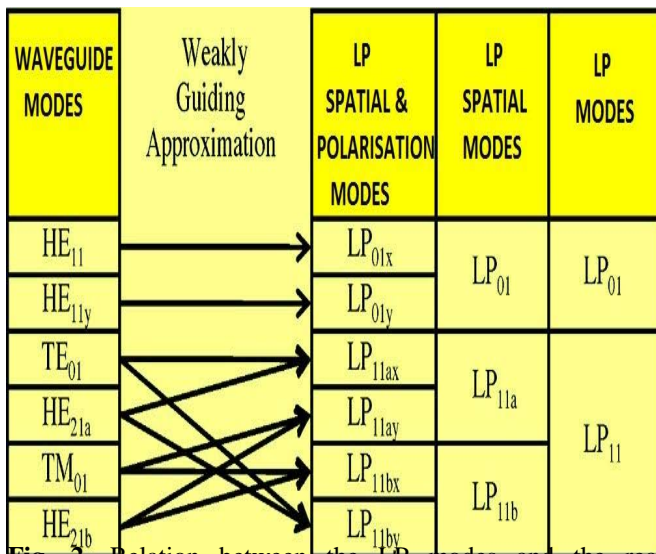

Fig. 2: Relation between the LP modes and the real waveguide modes HE_{11x}, HE_{11y}, TE_{01}, TM_{21a}, HE_{21a}, and HE_{21b} of the six-mode FMF.

The signals from N transmitters are coupled into the SDM fiber by an SDM multiplexer (SDM-MUX). After transmission through the SDM fiber, the received signals are demultiplexed by a SDM demultiplexer (SDM-DEMUX) and fed into N coherent receivers. The received signals are subsequently processed using MIMO DSP.

In order to achieve the full SDM capacity gain of a factor N at high reliability (i.e. low outage), it is required that the N N transmission channel consisting of SDM-MUX, SDM fiber, and SDM-DEMUX be described by a unitary linear transfer function [18]. In particular this requires that the SDM-MUX and DEMUX be capable of exciting all the modes supported by the SDM-fiber in a selective way. For the SDM fiber, the requirement implies negligible polarization dependent loss (PDL) and negligible mode-dependent loss (MDL). These conditions are fulfilled for both the FMF and CCF.

In this paper, we present SDM transmission over an FMF supporting six spatial- and polarization modes, referred in the following as six-mode FMF. In order to clarify our nomenclature of the modes, Fig. 2 lists the six fiber-waveguide modes of the six-mode FMF according to [19] and [20] on the first column, and its relation to the linearly polarized (LP) mode LP and the twofold degenerate LP mode listed in the forth column.

LP_{11a} and LP_{11b} are used to distinguish the degenerate LP_{11} mode, and the suffix x and y in the indexes are used to distinguish the two orthogonal linear polarizations.

The six-mode FMF allows for six independent data channels to be simultaneously transmitted at a single wavelength. The six data channels are launched polarization multiplexed into the LP_{01} , the LP_{11a} , and the LP_{11b} spatial mode, using a mode multiplexer with high mode selectivity (> 28dB). The mode multiplexer is based on phase masks fabricated in glass, which is a simple yet effective alternative to multiplexers based on programmable spatial light modulators.

The design offers low crosstalk and low polarization dependence. After transmission, a second mode multiplexer is used to separate the received optical field into three spatial channels that are detected by three synchronized coherent receivers with polarization diversity.

In order to recover the transmitted data, 6×6 MIMO DSP is applied to undo coupling effects occurring within the fiber. MIMO processing compensates linear impairments like dispersion, crosstalk, and DGD between modes and polarizations.

2. Space Division Multiplexing Over Few-Mode Fiber

The FMF used in this work is based on a depressed cladding index profile with normalized frequency V nearly = 5, where the normalized frequency is defined as

$$V = \frac{\pi d}{\lambda \sqrt{(n_1)^2 - (n_2)^2}}$$

where d is the core diameter, λ the wavelength of light and n1 and n2 are the refractive indices of core and cladding respectively.

The fiber was designed to guide exactly six polarization- and spatial-modes (The fundamental LP_{01} mode and the twofold degenerate LP_{11} mode), and also to minimize the modal DGD between the LP_{01} and LP_{11} across the C-band. The DGD has to be kept as small as possible, because any delay introduced between the SDM channels has to be compensated by means of filters with a correspondingly large memory as part of the MIMO DSP.
The fiber employed in our experiment [12] has a loss coefficient of 0.205 dB/km at 1550 nm and no significant mode-dependent loss. The effective areas of the LP_{01} and LP_{11} modes are approximately 155 and 159 m^2, respectively, and the chromatic dispersion is 18 ps/(nm km) for both LP_{01} and LP_{11} modes.

The DGD between the LP_{01} mode and the LP_{11} mode is to be measured by launching a 100-ps intensity-modulated probe pulse simultaneously into the LP_{01} and the LP_{11} spatial mode, and its value measured for a 96-km long FMF was found to be within 2.6 0.1 ns over the wavelength range of 1530 to 1565 nm, corresponding to a length specific DGD of 27 ps/km.

In comparison, the DGD of a step-index (SI) profile FMF with the same normalized frequency is 4300 ps/km, and therefore more than two orders of magnitude larger. Fiber with DGD even lower than 27 ps/km are highly desirable in order to further reduce the memory size required in the MIMO DSP.

In order to achieve the maximal SDM capacity gain, the complete set of modes supported by the 6-mode FMF has to be launched without significant crosstalk [18]. We therefore built spatial-mode multiplexers (MMUXs) to couple the light from three single-mode fibers into the different spatial modes of the 6-mode FMF.

A simple way to selectively couple light into a LP_{11} mode [21-22] ,where a phase plate having a phase profile matching the phase of the target mode is inserted into the optical path between the incoming SMF and the 6-mode FMF.
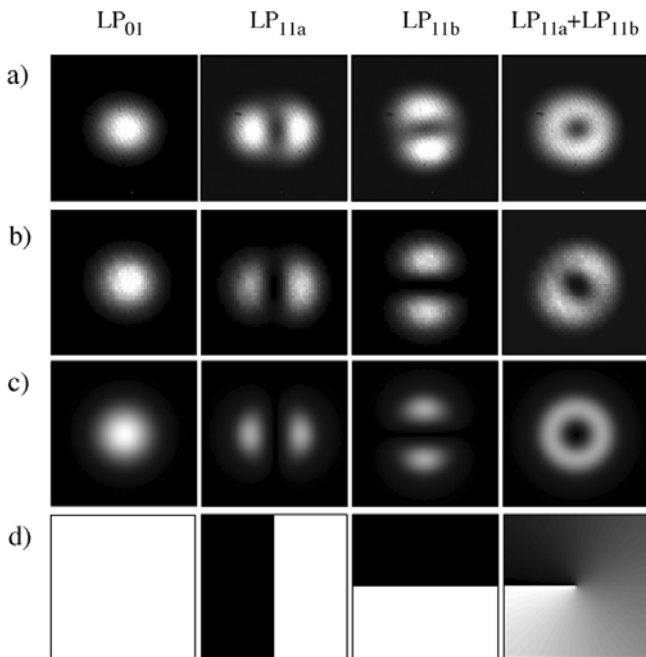

Fig. 3. Mode intensity profiles measured after a) 96-km and b) 33-km 6-mode FMF for different launched modes. c) Theoretical mode intensity profiles for a 6-mode FMF and d) corresponding phase profiles.

3. Overall System Model

A. Experimental Setup for SDM transmission
The SDM transmission-measurement setup is shown in Fig.4. The source signal for the experiment is generated by modulating an external cavity laser (ECL) at 1560-nm wavelength and having a linewidth of 100 kHz. The signal is modulated by a double-nested LiNbO3 Mach-Zehnder modulator using quadrature-phase-shift-keying (QPSK) where the in-phase (I) and quadrature (Q) components are driven by two independent De Bruijn bit sequences (DBBS) of length 2^{12}, respectively [23].

The use of two independent bit patterns offers the advantage of avoiding correlation effects[24-25]. Subsequently, a

polarization-multiplexing stage with a delay of 12 ns generates a PDM-QPSK signal which is followed by a noise - loading section consisting of a variable optical attenuator (VOA) in front of an Erbium-doped fiber amplifier (EDFA).

The PDM-QPSK signal is then split into three copies with a relative delay of 27 ns and 53 ns, that are connected to different SMF ports of the input MMUX. The MMUX is connected to the FMF fiber under test and a second MMUX acting as mode demultiplexer is used to terminate the FMF. The mode demultiplxed signals are then amplified using low noise EDFAs before being detected by three polarization-diversity coherent receivers (PD-CRX).

Each PD-CRX consists of a polarizing beam splitter (PBS) followed by two optical hybrids whose output ports are termi-nated by four balanced receivers. A second ECL is used as a local oscillator (LO) and the resulting 12 electrical high-speed signals from the PD-CRXs are captured using 3 high-speed digital oscilloscopes with 4 ports each, operating at a sampling rate of 40 GS/s. Each measurement consists of a total of four million samples captured using a common trigger signal.
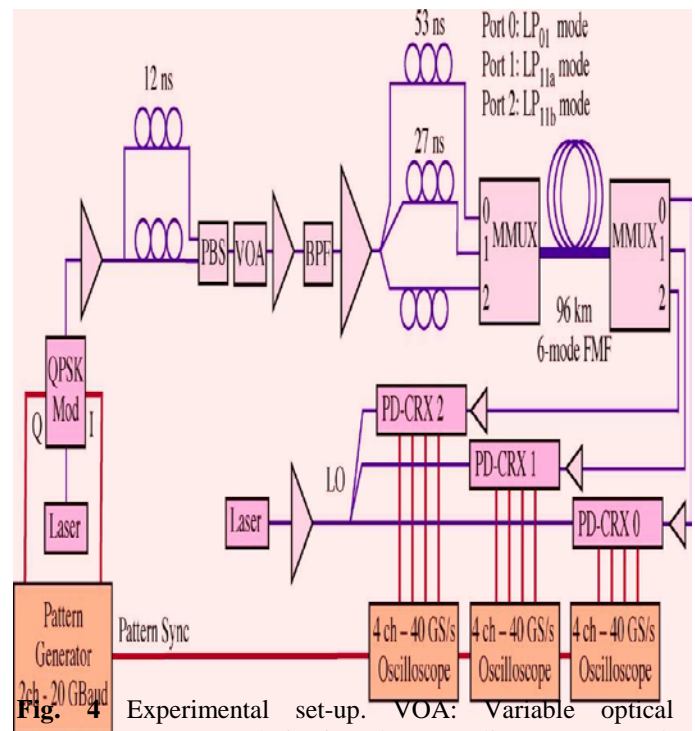

Fig. 4 Experimental set-up. VOA: Variable optical attenuator, PBS: Polarization beam splitter,QPSK-Mod: QPSK Modulator, BPF: Bandpass filter, LO: Local oscillator, PD-CRX: Polarization-diversity coherent receiver.

B. BER evaluation using MIMO DSP
The measurements are subsequently analyzed using off-line DSP. The 6×6 MIMO DSP architecture is an extension of the 2×2 implementation frequently found in coherent PDM receivers and is shown in Fig.6 (a) and (b). The six complex received signals r_{1-6} derived from the 12 electrical signals from the three PD-CRXs are fed into six column equalizers ($ceq_{1\ 6}$) (see Fig.6(a)). Each of the column equalizers produces a single output signal y_{1-6}.
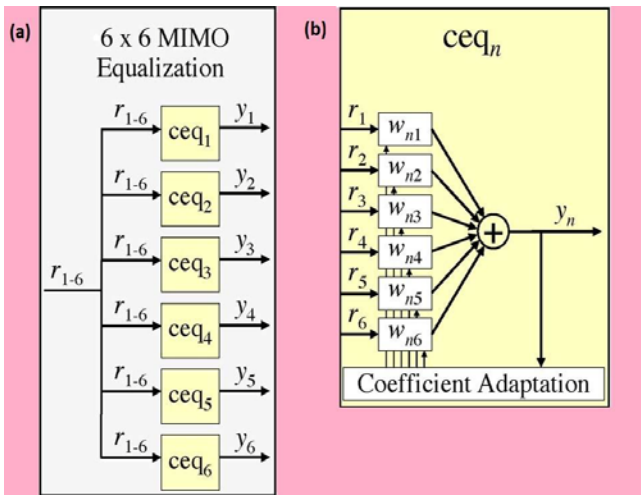
Fig 5. a) Architecture of the MIMO equalization block. b) Architecture a column equalizer ceqn.

The architecture of the column equalizer ceq_n is reported in Fig.5(b) and contains six feed-forward equalizers (FFEs). Each FFE has L taps associated with the complex coefficient vectors $w_{n1...n6}$ with length L. The recovered signal y_n is determined as the sum of the outputs of the 6 FFEs. The 6 6 MIMO DSP requires a total of 36 FFEs and the equalizer coefficients $w_{n1...n6}$ are optimized by applying the least-mean-square estimate (LMS) algorithm [26] modified to include carrier phase estimation (CPE) based on the fourth power algorithm [27].

In order to achieve initial convergence of the equalizer coefficients, the algorithm assumes knowledge of the received data (data aided) for the first 500,000 symbols, and later switches to a decision-directed LMS algorithm. Finally the bit-error rate (BER) is evaluated over the last one million bits of the acquired data.
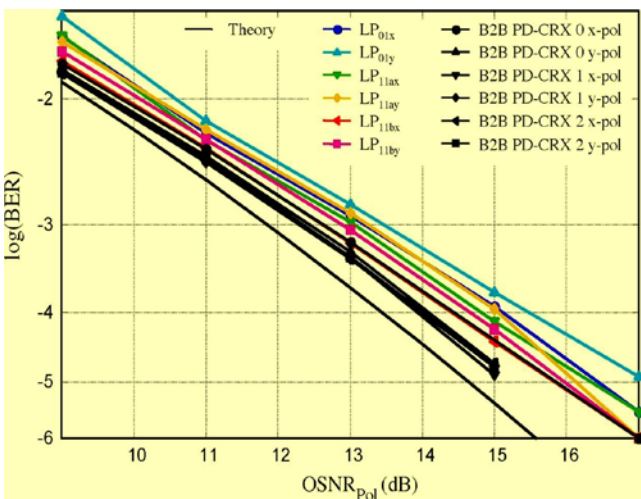

Fig. 6. BER curves for 6-channel PDM-SDM transmission of 20-Gbaud QPSK over 96 km of 6-mode FMF. Also shown for reference are the back-to-back measurements and the theoretical limit.

Fig.6 shows the experimental BER curves after off-line 6 6 MIMO processing with 120 taps, after transmission through 96 km of 6-mode FMF. All 6 transmitted data streams are successfully recovered by the MIMO DSP. The BER curves are plotted as a function of $OSNR_{pol}$, which is defined like the single-mode OSNR (using 0.1-nm optical noise reference bandwidth), but only the noise that is co-polarized with the corresponding signal component is included. Fig.6 also shows the theoretical limit for coherent detection of QPSK, and the back-to-back (B2B) measurements as a reference.

All B2B measurements show a penalty of less than 0.8-dB at a BER of 10^{-3}, and all 6 BER curves of the transmitted signals are within 1.2 dB from the back to back measurements. This excellent performance shows that crosstalk present in 96-km of 6-mode FMF can be successfully compensated with very low impact on system performance.
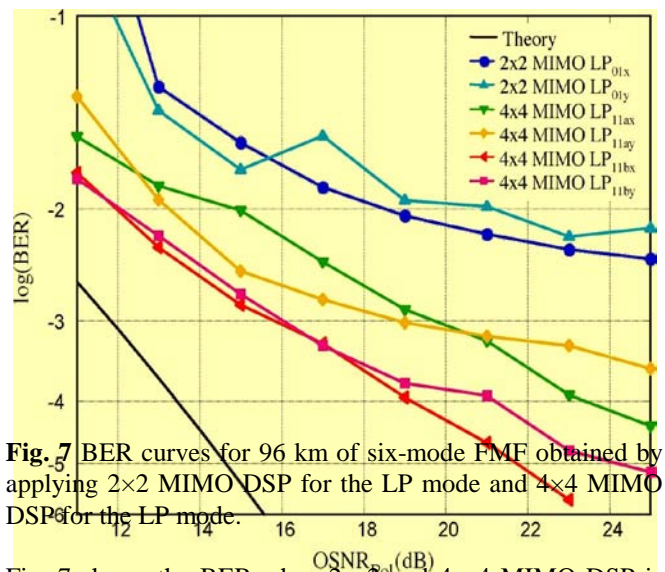

Fig. 7 BER curves for 96 km of six-mode FMF obtained by applying 2×2 MIMO DSP for the LP mode and 4×4 MIMO DSP for the LP mode.

Fig. 7 shows the BER when 2×2 and 4×4 MIMO DSP is used. The performance is dramatically degraded. A large penalty of 8 dB at a BER of 10^{-3} is observed for the LP_{11} mode, whereas a BER of 10^{-3} cannot be reached for the LP_{01} mode. Also we observe a large variability of the BER for different values of $OSNR_{pol}$, which we attribute to the fact that for each $OSNR_{pol}$ setting, measurements are taken several minutes apart from each other. Therefore, the crosstalk conditions, which are continuously changing in the fiber on a millisecond time scale, may have been different, leading to a variation in BER. Also, we would like to mention that this result is only valid for the low-DGD six-mode FMF used in this experiment. For FMF with larger modal propagation constant difference, a weaker coupling between the LP and the LP modes is predicted, and good performance can be expected.

C. Impulse-response matrix measurement of the 6-mode FMF

MIMO DSP techniques were applied to nullify linear distortions and crosstalk introduced by the FMF. In this section, we use MIMO DSP techniques to estimate the linear transfer

2nd International Seminar On "Utilization of Non-Conventional Energy Sources for Sustainable Development of Rural Areas
ISNCESR'16
17th & 18th March 2016

function of the FMF channel. The 6-mode FMF is equivalent to a 6×6 MIMO channel, which is fully characterized by its 6×6 impulse responses h_{nm}, where n is the index of the receive port and m is the index of the transmit port.

The squared magnitude of the 6×6 impulse responses are shown in Fig.8 for the 96-km long FMF. In this representation, each column corresponds to the impulse responses associated to a particular transmit port, whereas each row is associated to a particular receive port.

The determination of the impulse-response matrix is referred to as channel estimation in MIMO literature, and several algorithms are available [28]. The results presented in Fig.9 were obtained using a least-square-error (LSE) estimator [11].

In order to highlight the components of the impulse response due to mode coupling, chromatic dispersion of 96 18 ps/nm was electronically compensated on the received signal r_i (k) prior to estimating the impulse-response matrix. This allows to clearly identify the main coupling which appears as sharp peaks.

Fig.8 is divided into four regions identified as A, B, C, and D.
Region A consists of a 2 2 array located in the top left corner and is formed by the impulse-responses h_{11}, h_{12}, h_{21}, and h_{22}. Region A shows the coupling between the two polarizations of the fundamental mode (LP01).
Region B consists of the 4 4 array located on the bottom right corner and, comprising the impulse-responses h_{33}, h_{36}, h_{63}, and h_{66}. Region B represents the coupling between the spatial and polarization modes LP_{11a}, and LP_{11b}.

The remaining off-diagonal regions C and D, which are enclosed by (h_{13}, h_{16}, h_{23}, h_{26}), and (h_{31}, h_{32}, h_{61}, h_{62}), respectively, describe the crosstalk between LP_{01} and LP_{11} modes. In Fig. 9 strong coupling peaks appear in regions A and B, and typically 100 to 1000 times weaker, 2.6-ns wide distributed coupling is observed in regions C and D.

The width of the distributed coupling of regions C and D is consistent with the DGD of 96-km 6-mode FMF, and can be interpreted as coupling occurring at various locations along the fiber. In fact, because light traveling in the faster LP_{01} mode will arrive earlier than light traveling in the slower LP_{11} mode, the time of arrival can be used to predict the location of the coupling between LP_{01} and LP_{11} modes.

Note that also regions A and B show a weak distributed coupling next to the strong coupling peaks. This weaker distributed coupling represents light that couples back and forth between LP_{01} and LP_{11} or LP_{11} and LP_{01} modes, respectively.

Fig.8 also confirms the excellent alignment of the MMUX. Any misalignment in the phase plates would be immediately visible as narrow crosstalk peaks either at the beginning or at the end of the distributed coupling in regions C and D.

The impulse response matrix provides a clear picture of the MIMO channel, indicating location and amount of crosstalk introduced by the MMUX and the 6-mode FMF. It is therefore a very useful tool for fiber characterization, coupler optimization, and fault localization.
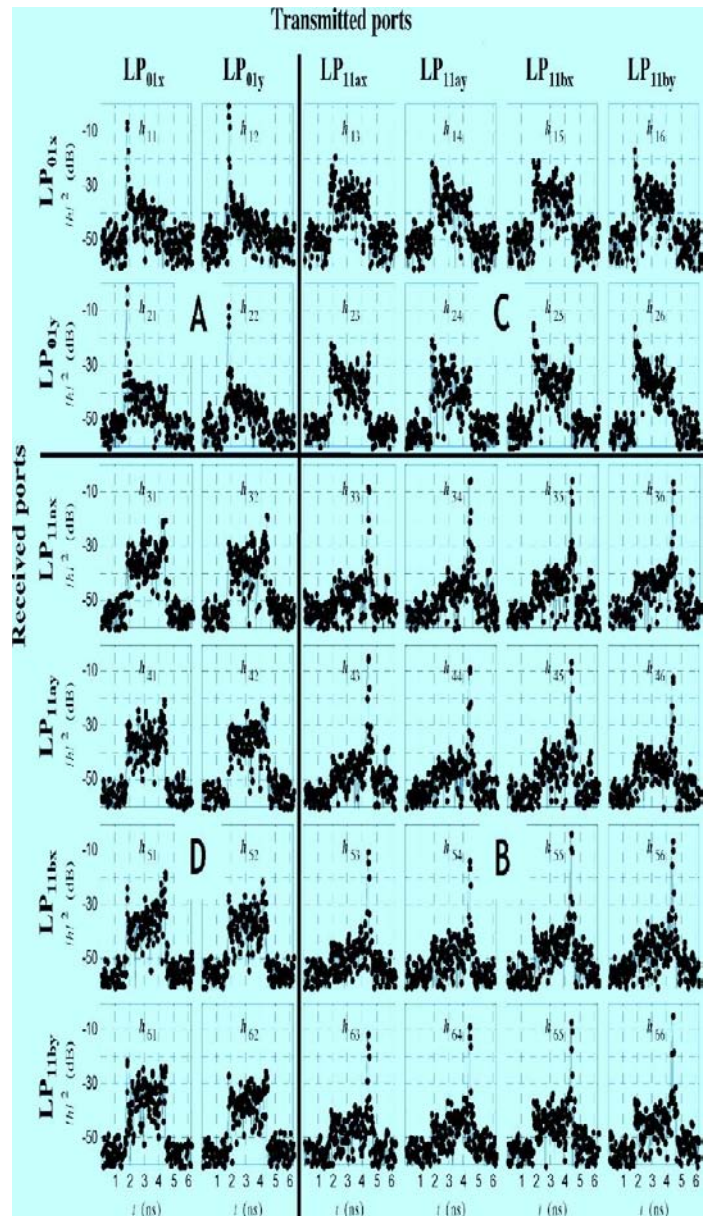

Fig. 8 Squared magnitude of the PDM-SDM 6 6 impulse responses for 96 km of six-mode FMF

4. CONCLUSION

In this paper, we understood that SDM transmission is possible in both multi-mode and multi-core fibers based on Multiple Input Multiple Output(MIMO) digital signal processing (DSP) systems. The results confirm that long haul transmission over both these fibers exist even in the presence of enhanced significantly large crosstalk between the SDM channels. Here, we also demonstrated single-wavelength as well as 6-channel spatial- and polarization-mode-multiplexed transmission of 6 40-Gb/s QPSK signals over 96-km of FMF with less than 1.2-dB penalty .The impulse-response matrix of the low-DGD FMF was described, revealing in detail the coupling between the six guided spatial and polarization modes. The results were obtained using offline coherent

2nd International Seminar On "Utilization of Non-Conventional Energy Sources for Sustainable Development of Rural Areas
ISNCESR'16
17th & 18th March 2016

MIMO DSP and highly efficient mode couplers based on phase plates.

Reference

[1] R. Tkach[1],(2010),"Scaling optical communications for the next decade and beyond," Bell Labs Technical Journal, vol.14 ,no.4 , pp.3 9.

[2] R.-J.Essiambre[1], G.Kramer[2], P. J. Winzer[3], G. J. Foschini[4], and B. Goebel[5] (2010), "Capacity limits of optical fiber networks," J. Light-wave Technol. vol.28, no. 4, pp. 662 701 .

[3] A.Chraplyvy[1] (2009), "The coming capacity crunch," Proc. European Conf. on Opt. Commun. (ECOC), Planary talk.

[4] P. J. Winzer[1] (2011), "Energy-efficient optical transport capacity scaling through spatial multiplexing," Photon. Technol. Lett. vol.23, no.13, pp.851 853 .

[5] S.Berdague[1] and P.Facq[2] (1982), "Mode division multiplexing in optical fibers," Appl. Opt. 21(11), 1950 1955.

[6] M.de Boer[1], C. P.Tsekrekos[2], A. Martinez[3], H. Kurniawan[4], , J. W. M. Bergmans[5], A. M. J. Koonen[6], H. P. A.van den Boom[7], and F. M. J.Willems[8], (2005), "A first demonstrator for a mode group diversity multiplexing communication system," in [Proc. IEE Seminar (Ref Optical Fibre Communications and Electronic Signal Processing No. 2005-11310)].

[7] S.Schollmann[1], S.Soneff[2], and W.Rosenkranz[3] (2007), "10.7 Gb/s over 300 m GI-MMF using a 2 2 MIMO system based on mode group diversity multiplexing," in [Proc. Conf. Optical Fiber Communication and the National Fiber Optic Engineers Conf. OFC/NFOEC 2007], pp.1 3.

[8] A.R.Shah[1], R. C. J. Hsu[2], A.Tarighat[3], A. H.Sayed[4] and B.Jalali[5] (2005), "Coherent optical MIMO (COMIMO)," J. Lightwave Tech-nol.,vol.23 ,no.8 , pp.2410 2419 .

[9] A.Li[1], A.Al Amin[2] , X.Chen[3] and W.Shieh[4] (2011), "Reception of mode and polarization multiplexed 107Gb/s CO-OFDM signal over a two-mode fiber," Proc. Opt. Fiber Commun. Conf. (OFC) , PDPB8 .

[10] M.Salsi1, C.Koebele2 , D.Sperti3, P.Tran4 , P.Brindel5 , H.Mardoyan6 , S.Bigo7 , A.Boutin8 , F.Verluise9 , P.Sillard10 , M.Bigot-Astruc11 , L.Provost12 , F.Cerou13 and G.Charlet14, (2011), "Transmission at 2×100Gb/s, over two modes of 40km-long prototype few-mode fiber, using LCOS based mode multiplexer and demultiplexer," Proc. Opt. Fiber Commun. Conf. (OFC) , PDPB9 .

[11] N.Hanzawa1 , K.Saitoh2 , T.Sakamoto3 , T.Matsui4 , S.Tomita and M.Koshiba6 (2011), "Demonstration of mode-division multiplexing transmission over 10 km two-mode fiber with mode coupler," Proc. Opt.Fiber Commun. Conf. (OFC) , OWA4.

[12] R.Ryf1 , S.Randel2, A. H.Gnauck3, C.Bolle4 , A.Sierra5 and S.Mumtaz6 , M.Esmaeelpour7 , E. C.Burrows8 , R.-J.Essiambre9 , P. J.Winzer10 , D. W.Peckham11 , A. McCurdy12 , and R. Lingle13 (2011), "Mode-division multiplexing over 96 km of few-mode fiber using coherent 6×6 MIMO processing," J. Lightwave Technol., special issue about OFC/NFOEC .

[13] E.Ip1 , N.Bai2 , Y.-K. Huang3 , E. Mateo4 , F. Yaman5, S. Bickham7 , S. Ten8 , J.Linares9, C.Montero10 , V.Moreno11 , X.Prieto12 , V. Tse13 , K. M. Chung14 , A. Lau15 , H.-Y. Tam16 , C. Lu17 , Y. Luo18 , G.-D. Peng19 and G. Li20 (2011), "88×3×112-gb/s WDM transmission over 50 km of three-mode fiber with inline fewmode fiber amplifier," Proc. European Conf. on Opt. Commun. (ECOC), Postdeadline , Th.13.C.2 .

[14] C. Koebele1 , M. Salsi2 , L. Milord3 , R. Ryf4 , C. Bolle5 , P. Sillard6 , S. Bigo7 and G. Charlet8 (2011), "40km transmission of five mode division multiplexed data streams at 100Gb/s with low MIMODSP complexity," Proc. European Conf. on Opt. Commun. (ECOC), Postdeadline paper , Th.13.C.3.

[15] R. Ryf1, A. Sierra2 , R.-J. Essiambre3 , S. Randel4 , A. Gnauck5 , C. Bolle6 , M. Esmaeelpour7 , P. Winzer8 , R. Delbue9, P. Pupalaiikise10 , A. Sureka11 , D. W. Peckham12 , A. McCurdy13, and R. Lingle Jr.(2011), "Mode-equalized distributed Raman amplification in 137-km few-mode fiber," Proc. European Conf. on Opt. Commun. (ECOC), Postdeadline Paper , Th.13.K.5.

[16] B. Zhu1 , T. F. Taunay2 , M. Fishteyn3 , X. Liu4 , S. Chandrasekhar5 , M. F. Yan6 , J. M. Fini7 , E. M. Monberg8 , and F. V. Dimarcello9, (2011), "Space-, wavelength-, polarization-division multiplexed transmission of 56 Tb/s over a 76.8km seven-core fiber," Proc. Opt. Fiber Commun. Conf. (OFC) , PDPB7.

[17] J. Sakaguchi1 , Y. Awaji2 , N. Wada3 , A. Kanno4 , T. Kawanishi5 , T. Hayashi6 , T. Taru7 , T. Kobayashi8 and M. Watanabe9 (2011), "109Tb/s (7_97_172Gb/s SDM/WDM/PDM) QPSK transmission through 16.8km homogeneous multi-core fiber," Proc. Opt. Fiber Commun. Conf. (OFC) , PDPB6 .

[18] P. J. Winzer1 and C. J. Foschini2 (2011), "MIMO capacities and outage probabilities in spatially multiplexed optical transport systems," Optics Express vol.19, no.17 , pp.16680□16696.

[19] G. Keiser (2000), Optical Fiber Communications, 3rd ed. New York: Mc- Graw Hill.

[20] D. Marcuse(1991), Theory of Dielectric Optical Waveguides, P. F. Liao and P. L. Kelley, Eds. New York: Academic.

[21] W. Q. Thornburg1, C. B. J.2 and X. D. Zhu3 (1994), "Selective launching of higher-order modes into an optical fiber with an optical phase shifter," Opt. Lett. vol.19 ,no.7, pp.454-456 .

[22] W. Mohammed1, M. Pitchumani2 , A. Mehta3 and E. G. Johnson4 (2006), "Selective excitation of the LP11 mode in step index fiber using a phase mask," Optical Engineering, vol.45, no.7 , pp.074-602

[23] Roland Ryf1, Sebastian Randel2, Rene-Jean Essiambre3 and Peter J.Winzer4 (2012)," Space-Division Multiplexed Transmission Over Few- Mode- and Coupled-Core Fiber Based on Coherent MIMO Digital Signal Processing," Bell Labs Technical Planary paper.

[24] A. Sierra1 , S. Randel2 , P. J. Winzer3 , R. Ryf4 , A. H. Gnauck5 and R.-J. Essiambre6 "On the use of delaydecorrelated I/Q test sequences for QPSK and QAM signals," Submitted to Photon. Technol. Lett. .

[25] S. Randel1 , R. Ryf2 , A. Sierra3 , P. J. Winzer4 , A. H. Gnauck5 , C. A. Bolle6 , R.-J. Essiambre7 , D. W. Peckham8, A. McCurdy9 , and R. Lingle10 (2011), "6_56-Gb/s mode-division multiplexed transmission over 33-km few-mode fiber enabled by 6_6 MIMO equalization," Optics Express vol.19, no.17, pp.16697□16707 .

[26] N. Benvenuto1 and G. Cherubini2 (2002), [Algorithms for communications systems and their applications], Wiley.

2nd International Seminar On "Utilization of Non-Conventional Energy Sources for Sustainable Development of Rural Areas
ISNCESR'16
17th & 18th March 2016

[27] A. J. Viterbi1 and A. M. Viterbi2 (1983), "Nonlinear estimation of PSKmodulated carrier phase with application to burst digital transmission,"

Author's Profile

Anuja Mishra is currently pursuing her M.E. Degree in the Department of Communication Engineering from Chhattisgarh Swami Vivekanand Technical University, Bhilai, India. She received her B.E. Degree in Electronics and Telecommunication Engineering from the Chhattisgarh Swami Vivekanand Technical University, Bhilai, India in 2014. Her current research interests are Photonics, Non Linear Fiber Optics and Optical Communication.

Sharad Mohan Shrivastava is currently working as an Assistant Professor in the Department of Electronics and Tele-communication at Faculty of Engineering and Technology, Shri Shankarachrya Technical Campus Bhilai, India. He received his B.E. Degree in Electronics and Communication Engineering from the Rajiv Gandhi Proudyogiki Vishwavidyala, Bhopal, India in 2009 and the M.E. degree in Electrical Communication Engineering from the Indian Institute of Science Bangalore, Karnataka in 2014. His current research interests are Photonics, Non Linear Fiber Optics and Optical Communication.